

# Reducing the first-order Doppler shift in a Sagnac interferometer

S. Hannemann,\* E. J. Salumbides, and W. Ubachs

Laser Centre, Department of Physics and Astronomy, Vrije Universiteit, De Boelelaan 1081, 1081 HV Amsterdam, The Netherlands

\*Corresponding author: shannemann@gmail.com

Received December 18, 2006; accepted January 16, 2007;  
posted March 14, 2007 (Doc. ID 78191); published April 25, 2007

We demonstrate a technique to reduce first-order Doppler shifts in crossed atomic/molecular and laser beam setups by aligning two counterpropagating laser beams as part of a Sagnac interferometer. Interference fringes on the exit port of the interferometer reveal minute deviations from perfect antiparallelism. Residual Doppler shifts of this method scale with the ratio  $v/(4d)$  of the typical atomic/molecular velocity  $v$  and the laser beam diameter  $d$ . The method is implemented for precision frequency calibration studies at deep-UV wavelengths, both in one- and two-photon excitation schemes: the  $6s^2 \rightarrow 6s30p_{3/2}$   $J=1$  line in Yb at 199 nm and the  $4p^6 \rightarrow 4p^5p[1/2]_0$  transition in Kr at  $\lambda=212$  nm. The achieved precision of  $6 \times 10^{-10}$  is limited by the characteristics of the laser system. © 2007 Optical Society of America

OCIS codes: 300.6360, 120.3180, 120.6200.

The Doppler effect, giving rise to line broadening and shifting, is an inherent obstacle in precision spectroscopy. In the past a number of Doppler-free techniques were developed to reduce or eliminate those influences [1]. Doppler-free saturated absorption spectroscopy [2] has become a standard method for absolute calibration of continuous-wave frequencies to sub-MHz precision. Doppler-free polarization spectroscopy [3], where a circularly polarized pump beam causes a birefringence in a gaseous medium, tilting the polarization of a counterpropagating linearly polarized probe beam, can be considered a variant of the same concept. Other techniques are based on multiphoton excitation, most prominently, Doppler-free two-photon spectroscopy [4].

Atomic and molecular beams are a widespread means to reduce Doppler broadening. Here it is essential to align the laser excitation beam under perfect perpendicular angle to reduce Doppler shifts in the spectroscopy. A method to solve this problem is to use a pair of counterpropagating laser beams and optimize their overlap such that both beams are subject to identical Doppler shifts with opposite signs. Moreover, when applying Doppler-free techniques, e.g., Doppler-free two-photon spectroscopy, saturable absorption or polarization spectroscopy, on atomic or molecular samples with anisotropic velocity distribution (such as in beams), the Doppler-free signal can be Doppler shifted within the bandwidth of the excitation light, when the beams are not perfectly antiparallel. Under such conditions, the attainable precision is restricted by the accuracy of the alignment procedure.

In the following, we demonstrate a method to reduce experimental Doppler-related uncertainties in atomic and molecular spectroscopy based on a Sagnac interferometer. Originally designed for rotation sensing [5,6], Sagnac interferometers were since then employed in a wide variety of laser-based applications. Here, a Sagnac interferometer is used to align two counterpropagating beams to high precision. We

demonstrate the technique for single-photon and Doppler-free two-photon excitation. Doppler uncertainties were reduced to the  $10^{-10}$  accuracy level.

A generic atomic or molecular beam experimental apparatus with the interaction zone placed in a Sagnac interferometer is depicted in Fig. 1. When the interferometer is aligned, two-beam interference is observed—parallel fringes with a periodic distance  $p$  and an inclination depending on the size and the orientation of the angle  $\delta$  between the two branches in the ring interferometer. An important advantage of such a ring interferometer is its stability with respect to acoustic perturbations: since the two interfering beams follow identical paths in opposite directions, the identical effects cancel out. Moreover, even if the coherence length of the laser light is short compared with the ring perimeter, fringes are still observable.

In a two-beam interference fringe pattern, the fringe period  $p = \lambda / \sin \theta$  is determined by the angle  $\theta$  between the two beams and the wavelength  $\lambda$ . In Fig.

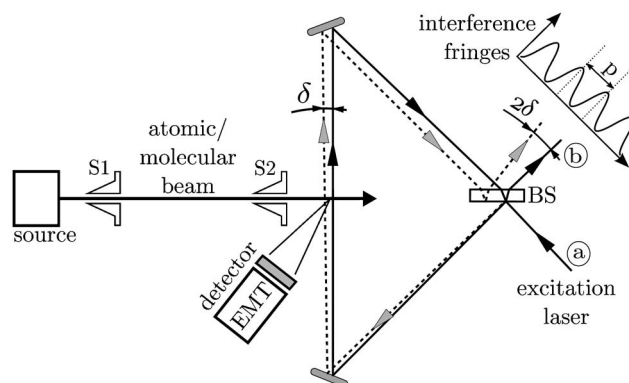


Fig. 1. Generic atomic/molecular beam setup combined with a Sagnac interferometer. A skimmed beam crosses two counterpropagating laser beams in the interaction zone. The incident light coming from port (a) follows the solid line in either direction when the ring is perfectly aligned. If one mirror is tilted by  $\delta/2$ , here the beam splitter (BS), the clockwise and counterclockwise beams generate a fringe pattern as depicted at port (b).

1 it is illustrated how  $\theta$  is related to the angular mismatch  $\delta$  of the counterpropagating beams inside the interferometer: The identical counterpropagating beam paths in a perfectly aligned interferometer are depicted as a solid line. The dashed line shows the beam that is reflected by a beam splitter tilted by an angle  $\delta/2$ . The transmitted beam, however, is only transversely shifted and follows the same direction as the beam of the perfectly aligned Sagnac interferometer. Hence, the angle between transmitted and reflected beam in the ring is  $\delta$ . When the reflected beam leaves the interferometer after being reflected by the beam splitter, it picks up another angular shift by  $\delta$  so that an angle  $\theta=2\delta$  defines the fringe period on the screen. The same result holds for any mirror tilted by  $\delta/2$  within the ring interferometer.

Consequently, the fringe periodic distance  $p$  increases for smaller  $\delta$ . In practice the interferometer is aligned until a dark fringe is achieved at port (b) and a bright fringe at port (a). This is due to the beam-splitting interface, at which the transmitted beam suffers no phase shift. The reflected beam, on the other hand, obtains a phase shift  $\pi$  at the first reflection at the beam splitter, but it does not when it is reflected the second time toward port (b). Achieving “dark fringe” condition means that  $p$  is larger than the beam diameter  $d$ . Accordingly, a large laser beam diameter helps for a precise alignment. If under experimental conditions the dark fringe alignment does not drift further than to the appearance of the first-order bright fringe, it is valid to state

$$2\delta = \theta \approx \sin \theta = \lambda/p < \lambda/d \quad (1)$$

as a conservative estimate for the deviation of  $\delta$  from zero. For a final frequency uncertainty resulting from the angular uncertainty  $\delta$ , an atomic beam of velocity  $v$  is considered at nearly perpendicular alignment with respect to the two counterpropagating laser beams of the ring interferometer. For one-photon excitation, the spectra from the counterpropagating arms are registered separately; after the ring interferometer is aligned and dark fringe is achieved, the light of one branch is blocked and the spectrum from the other beam is acquired and vice versa. The error  $\Delta f$  on the Doppler-free frequency calculated from the two spectra can be estimated from the error in  $\delta$  using Eq. (1) by inserting into the following:

$$\Delta f = \frac{v}{\lambda} \sin \frac{\delta}{2} < \frac{v}{4d}. \quad (2)$$

The Sagnac alignment method is demonstrated for single-photon excitation laser-induced fluorescence (LIF) and two-photon resonantly enhanced multiphoton ionization spectroscopies on atomic beams (for the setup see Fig. 1). The laser system employed, providing the fourth harmonic of an injection-seeded titanium:sapphire (Ti:Sa) narrowband oscillator (pulse length 25 ns, linewidth  $\approx 20$  MHz) has been documented before [7], as well as the application in one-photon [8] and two-photon [9] spectroscopies. The absolute calibration is performed on the seed light from a Coherent 899 (Ti:Sa) ring laser using a femtosecond

frequency comb. To exclude any ambiguity on the choice of the right mode number of the frequency comb, a saturable absorption  $I_2$  spectroscopy setup is available for precalibration and its use for the Yb spectroscopy is shown in Fig. 2. Frequency offsets between seed light and output of the pulsed oscillator—caused by frequency chirp and mode pulling—are taken into account by an online chirp analysis [9].

For demonstration in a one-photon LIF experiment the  $6s^2 \rightarrow 6s30p_{3/2}$   $J=1$  line in YbI is investigated. Figure 2 shows an overview recording for seven Yb isotopic lines, as well as a highly resolved spectrum of  $^{74}\text{Yb}$  at a width of 43 MHz. The precision calibrations for Yb, as listed in Table 1, are obtained from averaging over LIF measurements for each of the counterpropagating laser beams crossing the Yb atomic beam. An analysis of the uncertainty budget is presented in Table 2. A similar precision calibration was performed on the  $3s^2 \ ^1S \rightarrow 3s4p \ ^1P$  line in Mg I at an accuracy of 1 MHz [8].

Two-photon Doppler-free spectroscopy on atomic beams is also affected by Doppler shifts when the counterpropagating beams are not perfectly antiparallel. The frequency deviation  $\Delta f$  on the two-photon level is a factor of 2 larger than given in Eq. (2). In this excitation scheme both beams are present in the interaction volume, so a single scan yields a Doppler-free value. The signal is obtained by ionized product extraction using a time-of-flight setup. Two-photon spectroscopy was performed on the  $4p^6 \rightarrow 4p^5p[1/2]_0$

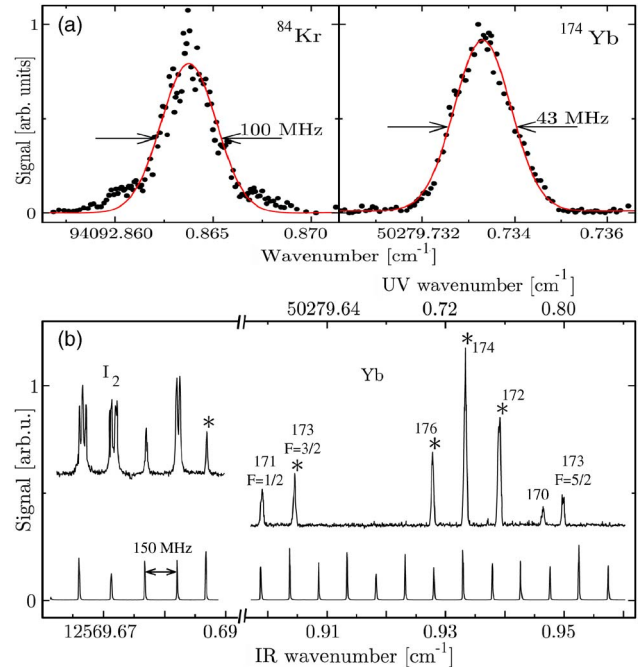


Fig. 2. (Color online) (a) Frequency comb calibration of the  $4p^6 \rightarrow 4p^5p[1/2]_0$  two-photon transition in  $^{84}\text{Kr}$  and the  $6s^2 \rightarrow 6s30p_{3/2}$   $J=1$  transition in the main Yb isotope. (b) Overview of the  $6s^2 \rightarrow 6s30p_{3/2}$   $J=1$  transition in Yb: a precalibration was performed using the b-component (marked with an asterisk) of the P(200) line of the B-X (0–14) band in  $\text{I}_2$  at  $12569.68739 \text{ cm}^{-1}$ . Frequency comb calibrations are performed for Yb isotopic lines marked with an asterisk.

**Table 1. Results of the Absolute Calibrations**

Species	# Scans	Position (cm <sup>-1</sup> )
<sup>84</sup> Kr	20	94092.86387(25)
<sup>172</sup> Yb	2·2	50279.711932(60)
<sup>174</sup> Yb	8·2	50279.733339(33)
<sup>176</sup> Yb	2·2	50279.755754(60)
<sup>173</sup> Yb	2·2	50279.620239(80)

**Table 2. Error Budgets for Each Species (in MHz)**

Uncertainty	Kr	<sup>174</sup> Yb	Other Yb
First-order Doppler	0.1	0.1	0.1
Frequency comb	<0.1	<0.1	<0.1
Chirp	4	0.5	0.5
Fit	3	0.5	2
AC-Stark	0.4	<0.1	<0.1
Total	6	1	2

line in krypton. Calibration results are also displayed in Tables 1 and 2. Since the laser beam is collimated to about 1 mm diameter, the estimated accuracy of the beam overlap for 200 nm light is better than 0.1 mrad according to Eq. (2).

The uncertainties of the frequency calibrations resulting from the first-order Doppler effect depend on the typical beam velocities. For both cases (Yb and Kr) it is estimated to be smaller than 100 kHz. The dominating uncertainties in these experiments result from the characteristics of the laser output, most notably the frequency chirp, which depends on the pump energy applied on the pulsed oscillator and on the seeding wavelength. For the Kr spectroscopy a seeding wavelength of  $\lambda = 850$  nm is used, which gives rise to more pronounced frequency chirp as at wavelengths  $\lambda = 800$  nm used for the Yb. To reduce chirp influences on the Kr calibration, the pulsed oscillator was operated at low pulse energies, which in turn increased the statistical fluctuations of the laser output energies and leads to a somewhat greater fit uncertainty.

The obtained transition frequency for the <sup>84</sup>Kr line  $\bar{\nu} = 94092.86387(25)$  cm<sup>-1</sup> is in good agreement with Witte *et al.* [10], who measured 94092.86399(12) cm<sup>-1</sup>, and with Brandi *et al.* [11], who provided a calibration for <sup>86</sup>Kr. Taking the accurately measured isotopic shift  $\nu_{86} - \nu_{84} = 135.99(17)$  MHz from Witte *et al.* into account, the calibration by Brandi *et al.* corresponds to

94092.8627(13) cm<sup>-1</sup> for <sup>84</sup>Kr, well within the specified confidence intervals.

In conclusion, Sagnac interferometry is an elegant technique to align two counterpropagating beams to exactly overlap. Calibration errors due to Doppler shifts in crossed beam configurations were reduced below the intrinsic accuracy limitations of the excitation laser system. The  $6s^2 \rightarrow 6s30p_{3/2}$   $J=1$  transition for <sup>174</sup>Yb was calibrated to the  $6 \times 10^{-10}$  accuracy level. The alignment precision is limited by the beam diameter of the excitation laser and can be improved by using larger diameters. Further improvement of the method can be accomplished by combining a fringe detection system with piezo actuators in an electronic feedback loop. The Sagnac interferometric method is especially useful, where “classical” methods of Doppler reduction fail. Additionally, no fiber coupling is involved, hence the method can be used for deep-UV light as demonstrated. The Sagnac interferometer produces fringes even for light exhibiting short coherence lengths, which potentially makes it useful for quantum interference spectroscopies as presented in Witte *et al.* [10] at deep-UV wavelengths and by Zinkstok *et al.* [12] in the VUV. The Netherlands Foundation for Fundamental Research on Matter (FOM) is gratefully acknowledged for financial support.

## References

1. W. Demtröder, *Laser Spectroscopy*, 3rd ed. (Springer, 2002).
2. R. L. Barger and J. L. Hall, Phys. Rev. Lett. **22**, 4 (1969).
3. C. Wieman and T. W. Hänsch, Phys. Rev. Lett. **36**, 1170 (1976).
4. B. Cagnac, G. Grynberg, and F. Biraben, J. Phys. (France) **34**, 845 (1973).
5. G. Sagnac, Compt. Rend. **157**, 1410 (1913).
6. E. J. Post, Rev. Mod. Phys. **39**, 475 (1967).
7. M. Snee, S. Hannemann, E. van Duijn, and W. Ubachs, Opt. Lett. **29**, 1378 (2004).
8. S. Hannemann, E. Salumbides, S. Witte, R. T. Zinkstok, K. S. E. Eikema, and W. Ubachs, Phys. Rev. A **74**, 012505 (2006).
9. S. Hannemann, E. Salumbides, S. Witte, R. T. Zinkstok, K. S. E. Eikema, and W. Ubachs, Phys. Rev. A **74**, 062514 (2006).
10. S. Witte, R. Zinkstok, W. Ubachs, W. Hogervorst, and K. Eikema, Science **307**, 400 (2005).
11. F. Brandi, W. Hogervorst, and W. Ubachs, J. Phys. B **35**, 1071 (2002).
12. R. T. Zinkstok, S. Witte, W. Ubachs, W. Hogervorst, and K. S. E. Eikema, Phys. Rev. A **73**, 061801(R) (2006).